FINAL REPORT FOR
CRYSTAL GROWTH CONTROL: NCC3-209

Walter M.B. Duval *, Celal Batur +, Robert J. Bennett +

*** NASA Lewis Research Center, Cleveland, Ohio 44135**

+ Department of Mechanical Engineering, University of Akron, Akron, OH 44325-3903

ABSTRACT

We present an innovative design of a vertical transparent multizone furnace which can operate in the temperature range of 25 °C to 750 °C and deliver thermal gradients of 2 °C/cm to 45 °C/cm for the commercial applications to crystal growth. The operation of the eight zone furnace is based on a self-tuning temperature control system with a DC power supply for optimal thermal stability. We show that the desired thermal profile over the entire length of the furnace consists of a functional combination of the fundamental thermal profiles for each individual zone obtained by setting the set-point temperature for that zone. The self-tuning system accounts for the zone to zone thermal interactions. The control system operates such that the thermal profile is maintained under thermal load, thus boundary conditions on crystal growth ampoules can be predetermined prior to crystal growth. Temperature profiles for the growth of crystals via directional solidification, vapor transport techniques, and multiple gradient applications are shown to be easily implemented. The unique feature of its transparency and ease of programming thermal profiles make the furnace useful for scientific and commercial applications for the determination of process parameters to optimize crystal growth conditions.

1.0 INTRODUCTION

One of the fundamental variables in crystal growth applications is the tuning of the thermal gradient, we present an innovative multizone transparent furnace design which allows precise control of the thermal field. The features of the furnace, from the standpoint of technical merit, which make it attractive are its transparency and ease of programming the desired thermal profile. The transparency feature of the furnace lends it the commercial potential for on-line quality control of crystal growth. The scientific application of the furnace is crystal growth of acousto-optic optoelectronic materials such as lead and mercurous halides, nonlinear optics, photonics, low temperature semiconductors and organic crystals, which span the temperature range of 25 °C to 750 °C.

For applications to the growth of bulk single crystal growth, it has been widely recognized by many investigators [1-4] that the thermal field affects the crystalline quality. These applications stem primarily from crystals grown by directional solidification for which the macroscopic shape of the solid-liquid interface is used as feedback for quantification of the localized thermal gradient. Though planar interfaces are preferable from the standpoint of minimization of thermal stresses [1], a convex interface may be beneficial for some applications. Thus, there exists benefits for tailoring the thermal profile to achieve certain desired outcomes.

Traditionally, crystals are grown in a two zone Bridgman furnace which provides two temperature baths, a hot and a cold zone, with a thermal gradient between the two zones. Chang and Wilcox [4] showed that the sensitivity of the interface shape can be decreased by inserting a layer of insulation between the cold and hot zone. The insulated layer causes the heat transfer to be unidirectional near the solid-liquid interface; this results in a nearly flat interface. Although this approach is desirable, the insulation layer blocks the view of the solid-liquid interface, which results in the loss of vital information. We introduce the design of a transparent eight zone furnace which allows the tailoring of thermal gradients. Due to its versatility, multiple gradients can be achieved whereby the heat transfer can be made unidirectional over a segment, without the use of insulation, thus preserving the transparency of the furnace. In addition to directional solidification applications, this furnace is useful for crystal growth by the physical vapor transport process which requires a thermal profile with a "hump" used to prevent spontaneous nucleation. This thermal profile has been used by Hartmann and Schonherr [5, 6] to measure crystal growth rates by relaxation. We present the design of the furnace and show thermal profiles of interest for both directional solidification as well as physical vapor transport used in applications to grow crystals.

2.0 EXPERIMENTAL DESIGN

2.1 Innovative Furnace Design

The basic characteristic of a crystal growth furnace is a device that allows a uniform thermal gradient to be established inside an enclosure with optimum temperature stability. In addition, this device should allow a range of thermal gradients to be set-up in order to allow optimization of crystal growth parameters, an important feature for directional solidification applications [7, 8]. Through several iterations, Batur et. al. [9,10] , we have constructed an eight zone furnace, shown in Figure 1, that fulfills our objectives. This furnace consists of two concentric quartz cylinders (high optical grade quartz 'GE-214'), of height 52 cm, inner diameter of 4.3 cm with wall thickness 3mm, and outer diameter of outer cylinder of 6.8 cm with wall thickness of 2 mm . A spiral helical groove, of equal depth and width of 1.27 mm, is imbedded on the outer surface of the inner cylinder with constant pitch. The heating kanthal wires are imbedded as a continuous coil on the outer surface of the inner cylinder. This allows the heat flux to be nearly uniform azimuthally; in addition the quartz tube act as a low pass filter to damp high frequency noise from the power supply. The outer cylinder which acts as an insulator is split axially, thus consists of two sections which allows for ease of instrumentation. The connection from the furnace, approximately 1.25 to 2 cm from the outer cylinder, to the main power supply requires the joining of the kanthal wire to 99% pure nickel by butt welding. The lower resistance of the nickel minimizes heat loss to the ambient environment. The heating elements (A-1, Kanthal wire) are placed into the spiral ground groove of the inner cylinder in a manner which minimizes the gap between heating elements.

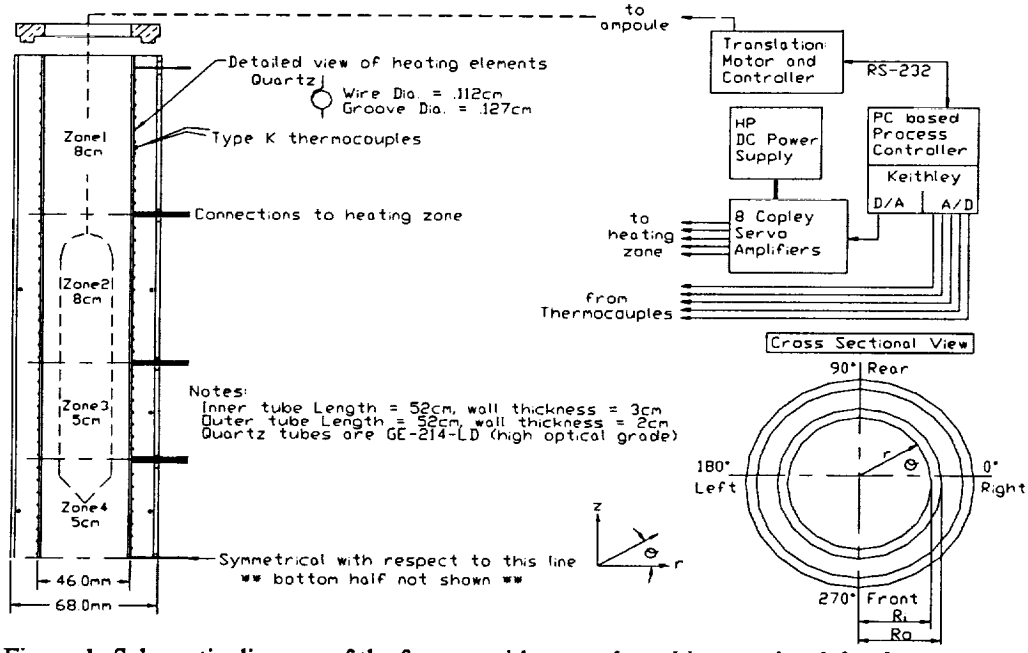

Figure 1- Schematic diagram of the furnace with ampoule and its associated hardware, cross sectional view shows location for wall temperature measurements.

The optimum length of the zones is selected to allow maximum power input for a given coil in order to achieve a certain temperature range. Whereas, the optimal pitch of the heater wires for each zone is selected such that maximum visibility is achieved through the heating coils. This feature makes the furnace useful for flow visualization studies as demonstrated by Lan et.al. [11]. The heating zone lengths necessary to meet our criteria are as follows: top and bottom zones of equal lengths $Z_1 = Z_2 = Z_7 = Z_8 = 8.0$ cm, and equal lengths of the inner four zones: $Z_3 = Z_4 = Z_5 = Z_6 = 5.0$ cm. This heating arrangement can provide an operating range from 25 °C to 750 °C and thermal gradients from 2 °C/cm to 45 °C/cm.

2.2 Temperature Control --- Hardware Implementation

The furnace zone temperatures are measured on the outside wall of the inner quartz tube with K type thermocouples. The thermocouple beads are of 0.5 mm in diameter and they are housed inside the small blind holes which are machined on the outside surface of the quartz tube. The positioning of thermocouples in this fashion insures that the beads are at equal distance from the centerline of the furnace. Therefore, the temperatures are controlled at equidistant locations with respect to the centerline. The measured temperatures are cold junction compensated and digitized by a Keithley analog to digital converter. The conversion resolution is 12 bits and, therefore, based on 0 - 1000 °C temperature range the smallest amount of temperature change that the measurement system can detect is about 0.25 °C.

The power inputs to heating zones are delivered through eight Copley servo power amplifiers. A 12 bit digital to analog (D/A) card from Keithley supplies a control voltage of 0 - 10 V to each servo amplifier. Since the D/A card is of 12 bits, a minimum amount of voltage change that the D/A card can send to the servo amplifier is about 2.5 mV. This effectively defines the resolution of the control signal. The servo amplifier can provide up to 500 W power to each heating zone. The gain of each amplifier is set to a level such that the (0- 10) V input from the D/A board corresponds to (0 - V_s) Volts where V_s is the supply voltage. There are two Hewlett Packard regulated DC power supplies, connected in parallel and providing up to 8000 W of power to heating zones through power amplifiers. The main advantage of using a DC power supply is the elimination of power supply induced disturbances. These disturbances are inherent to an AC power supplied furnace. This is due to the fact that there are basically two different ways that one can use to deliver the power from an AC source to the furnace in a regulated manner. One way is based on changing the power activation point within each cycle of the AC voltage. Since this implies a sudden current change to the heater within each cycle, the resulting effect is the electrical noise due to inductive effects. The second type of systems use zero crossing and duty cycle modulation where the duty cycle is defined as the ratio between the (power on) time to (power on + plus power off) time. Under this system, the heating zone effectively operates under ON-OFF control and if the duty cycle is small this ON-OFF type power regulation introduces its own disturbance into the thermal dynamics. The DC power supply completely eliminates the power supply induced disturbances. A schematic that shows the main features of the hardware is also given in Figure 1.

2.3 Temperature Control --- Software Implementation and Thermal Model

The temperature of each zone is controlled by a self-tuning PI (Proportional - Integral) control algorithm. There are two kind of disturbances that require the self-tuning control action. The first group is due to the motion of the ampoule and the interface which change the thermal dynamics of the heating zone because of changes of thermal inertia within the zone during motion. The second disturbance is caused by the inevitable zone to zone heat exchange since the heating zones are not thermally insulated. At each sampling instant the temperature control algorithm first updates the thermal model of the zone so that the current input output data fit the model in a least squares sense. We assume the following dynamic model for the purpose of controller design

$$T(t) = A.T(t-1) + B.u(t-1) + e(t) \quad (1)$$

Where $u,T \in R^8$ are the process inputs and the measured zone temperatures respectively and $e(t) \in R^8$ indicates the inevitable zone to zone thermal interaction on the temperatures. The matrices $A,B \in R^{8x8}$ define the thermal dynamics of the system. The process input is determined by the temperature controller and it is the energy flow into eight heating zones, i.e., $u=(u_1,u_2,\ldots,u_8)^T$. Once the thermal model is updated, the parameters of the PI controller is modified in order to take into account the most recent changes in thermal dynamics. The model updating is based on the multivariable Least Squares criterion, i.e., at each sampling instant the model matrices A and B are updated such that the residuals are minimum, i.e., the following identification performance index is minimum

$$V_{ID} = \text{trace}\{\arg_{\hat{A},\hat{B}} \min[\sum_{k=1}^{t} \hat{e}(k).\hat{e}^T(k)]\} \quad (2),$$

where the residual of the model is given by

$$\hat{e}(k) = T(t) - \hat{A}.T(t-1) - \hat{B}.u(t-1) \quad (3) \ .$$

The modification of the PI control parameters is based on the eigenvalue placement whereby the PI control parameters are changed such that the control system generates the fastest corrective response to the disturbances without causing overshoot or undershoot in the zone temperature. The details of the algorithm can be found in [12].

3.0 ENERGETICS AND MEASUREMENTS OF THERMAL PROFILES

3.1 Relationship between Set-points and Measured Temperatures

A given temperature profile in the furnace is established by setting eight discrete temperatures, T_1, T_2, T_3, ...T_8, at the midpoint of each zone on the outer surface of the inner cylinder. Previous designs in which holes were drilled along the axis of the inner tube suffered from significant heat loss which prevented a uniform thermal field inside the furnace. When a given zone, Z_i, is activated at a temperature T_i, the control system set-up a heat flux distribution, $q''(\theta,z)$ *at* $r = Ro$ on the outer surface of the inner cylinder. Some of this heat is lost and the remaining is transmitted inside the furnace which results in thermal equilibrium due to contributions of the heat flow modes, namely, conduction, convection , and thermal radiation. Since the temperature along the inside wall (r = Ri) can be readily measured, the imposed boundary condition may be denoted by the temperature distribution $T = T(r = R_i, \theta, z)$ instead of the heat flux. In order to ascertain the relationship between set-point temperatures and the temperatures inside the furnace, we use a calibrated NIST-Standard type S thermocouple to measure the thermal profile. Since we have air inside the furnace, fundamentally the temperature profile is influenced by buoyancy induced flows due to density gradients, this problem may be posed as follows:
For a set-point temperature, T_i which establishes a surface temperature

$$T=T(\theta,z) \text{ at } r=R_i, \quad (4),$$

along the inside wall of the inner cylinder for a given zone Z_i, buoyancy induced flows will ensue inside the furnace when the axial heat loss along the wall creates unstably stratified air layers. This heat loss causes a gaussian-like temperature distribution for the individual inner zones of the furnace Z_2-Z_7. The density of air, a homogeneous fluid, is a function of temperature and pressure,

$$\rho = \rho\left(P, T \right) \quad (5).$$

Within first order approximation the effect of pressure may be neglected so that,

$$\rho = \rho o + \frac{\partial \rho}{\partial T}\left(T - To\right) + \frac{1}{2!}\frac{\partial^2 \rho}{\partial T^2}\left(T - To\right)^2 + \ldots \quad (6).$$

The subscript o indicates a mean value, due to small variation of the density with temperature, second order derivatives and higher may be neglected. Regions in which the density field becomes unstably stratified, due to an adverse density field variation from equation 6, will give rise to a flow field which satisfies the conservation of mass, balance of momentum, and conservation of energy as follows:

$$\nabla \bullet \vec{V} = 0 \quad (7)$$

$$\rho_0 \frac{D\vec{V}}{Dt} = -\nabla P + \mu \nabla^2 \vec{V} + \rho\, \vec{g} \quad (8)$$

$$\frac{DT}{Dt} = \alpha\, \nabla^2 T \quad (9).$$

$\vec{V}$ represents the flow field, $\vec{g}$ is the gravitational acceleration, μ and α are the dynamic viscosity and thermal diffusivity of the fluid. The density field variation equation (6) gives the coupling between the energy equation (9) and the momentum equation (8). The solution to this problem can be determined numerically to obtain the temperature field inside the furnace ,

$$T=T(r, \theta, z, t), \quad (10)$$

as a predictive tool for a prescribed boundary condition. Alternatively, the temperature field can be measured to obtain the solution. In our case we measured the temperature field and found that azimuthal symmetry, i.e. T(r,z), in the gradient region for linear temperature profiles is a good approximation. Even though, there is a slight radial

dependence, the temperature profile at the centerline, T=T(z) at r=0, gives a good indication of the temperature gradient.

3.2 The elements of thermal profile

The measured centerline thermal profile consists of a functional combination of the profile of individual zones. Figure 2, shows the corresponding thermal profile for a set point temperatures of T=373 °C applied at each zone individually, the origin of the coordinate system is at the top of the furnace. These profiles correspond to one zone in operation, while keeping the other zones off. Since zone 1 is near the top, the heat loss near the top of the quartz tube is minimal. There is a local temperature maximum in zone 1 which decreases exponentially toward the bottom of the furnace. In contrast, note that heat loss, for all the zones, along the axial direction towards the top of the furnace increases as the zone distance from the top of the furnace increases. This effect of heat loss is augmented by the Rayleigh-Taylor instability which occurs due to unstable air density stratification, which is shown by the scatter of data near the top region, illustrated more clearly for zone 6. This convective flow situation denoted by $\vec{V}$ in equation (8) occurs because the air density decreases, above the location of the maximum temperature, for example zone 4; this provides a situation where a heavy air layer lies on top of a lighter layer which gives rise to a convective flow field. The scatter of the data as shown in zone 6 is attributed to this convective instability. On the other hand , note that toward the bottom of the furnace the temperature profile is smooth; this is because as the temperature decreases the lighter fluid air elements overlays the heavier elements which provide a stable situation. Thus, there is no convective flow. The gaussian-like wall temperature distribution as shown in our furnace has similar effect on driving buoyancy induced convection as the case of a heat source at the bottom of the furnace [13] in which the walls would either have a linear imposed temperature gradient or be insulated.

The temperature profiles in Figure 2 showed the one dimensional (1-D) behavior of the thermal field at the centerline, however, for a given axial location (z) it is likely that there exists 3-D thermal surfaces in the (r,θ) plane. In order to investigate this likelihood, in addition to the centerline we also probed the inside wall of the furnace to permit a 3-D reconstruction of the temperature field. In contrast to the measurements in Figure 2 which used an AC based power system (kanthal wire diameter .125cm), we switched to a DC based system with different kanthal heating wire diameter .081cm, hence different resistance. Using the same set-point as before 373 °C, we obtained the same trends in zone 4 shown in Figure 3, however, the magnitude of the response temperature in the furnace varied. The wall temperatures were measured at the z-plane which corresponds to 0° (Right), 90° (Rear),

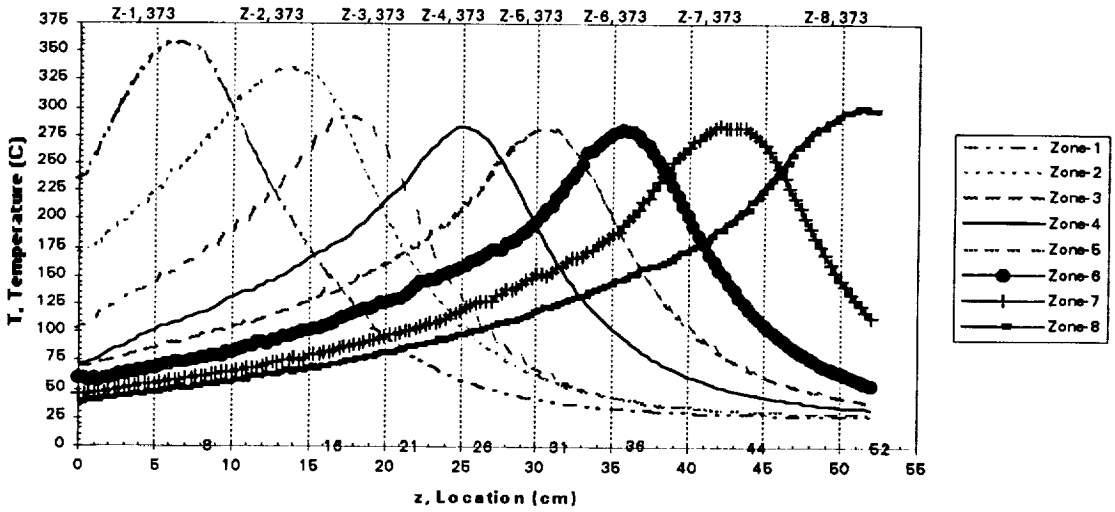

Figure 2- Thermal profile characteristics of the furnace illustrating the behavior of each zone for the same set-point temperature, T=373^{0}C. Top numerical numbers indicate zone set-point temperatures (^{0}C), bottom numbers inside plot indicate location of boundaries between zones.

180° (Left), 270° (Front), respectively as shown in Figure 1. The results show that maximum deviation from the centerline temperature occurs in the neighborhood of the local maximum z=25 cm of the thermal profile. A 3-D reconstruction shows that the thermal surface corresponds to a skewed paraboloid of revolution at z=25 cm. Note that near the top of the furnace z < 19 cm, the centerline temperature becomes higher than the wall temperatures. This trend is attributed to intense convective motion as we had discussed earlier. In contrast for z > 30 cm in which there is no convective motion, the centerline temperature is approximately the same as the wall temperatures. The isothermal surface for the location z = 35 cm would correspond to a skewed hemisphere, note that the centerline temperature is greater than most of the wall temperatures for this region. Much of the skewdness in the 3-D representation stems from the helical path of the heating wire which will inevitably cause local temperature nonuniformity on the wall of the furnace. Since the majority of practical thermal profiles for crystal growth is obtained by fixing a hot and a cold zone similar to the region z > 30 cm, the centerline temperature profile would give a good representation of the thermal gradient. Though, we have shown the furnace response when a single zone is activated, the effect of activating two or three zones simultaneously using the same set-point is to broaden the peak of the thermal profile such that a flat isothermal region is obtained.

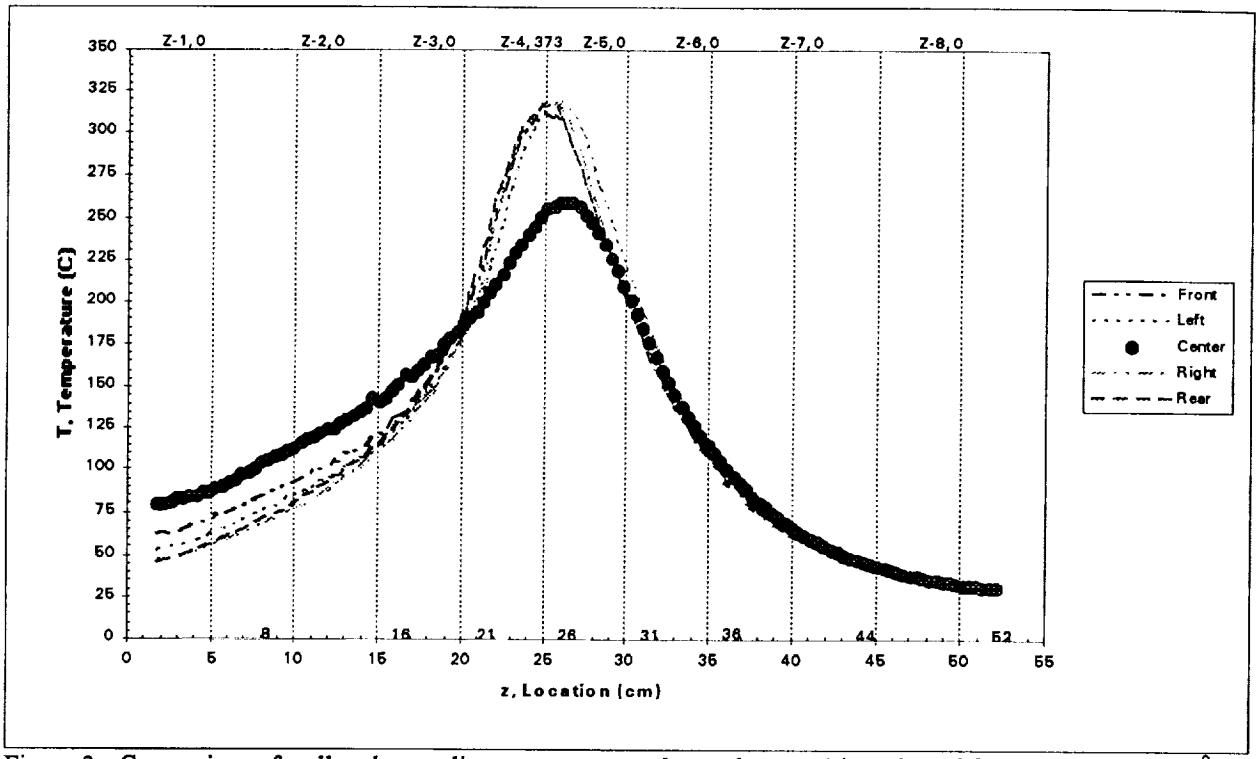

Figure 3 - Comparison of wall and centerline temperatures when only zone 4 is activated for a set-point of 373^{0}C. Set-point temperatures of 0 ^{0}C indicate no power supplied to zones.

Given the individual performance of the various zones, operation of all the zones in synchronization results in nearly isothermal conditions over a segment, 25cm $\leq z \leq$ 35cm, of the furnace shown in Figure 4. All the zones were set to the same temperature for each case, slight adjustments can be made to achieve the desired level of isothermality. Crystal growth under practical conditions requires specific thermal profiles, we show various profiles measured at the centerline as well as the wall to give an indication on how well the furnace projects the imposed thermal boundary conditions. An example of a linear thermal gradient is shown in Figure 5. This thermal gradient is necessary for the growth of crystals via directional solidification. The wall temperature gradient in the region of interest 16 cm $\leq z \leq$ 25 cm is approximately the same as that of the centerline (20 °C/cm) The growth of crystals by physical vapor transport necessitates a thermal profile with a "hump" shown in Figure 6. This case illustrates that maximum deviation of the thermal gradient occurs in the region of the "hump", 20cm $\leq z \leq$ 28 cm. The centerline temperature gradient for that region is 17°C/cm, whereas the average wall gradient is 31°C/cm. As we had discussed earlier, some applications necessitate localized heat transfer in one direction, the multiple gradient shown in Figure 7 is an alternative for obtaining the same effect as insulation while preserving the transparency of the furnace. The isothermal region occurs for 23 cm $\leq z \leq$ 29 cm, and centerline thermal gradients of 25 °C/cm and 20 °C/cm corresponding to the regions 15 cm $\leq z \leq$ 20 cm and 30cm $\leq z \leq$ 39cm respectively. There is good agreement between the wall and centerline temperatures for those regions.

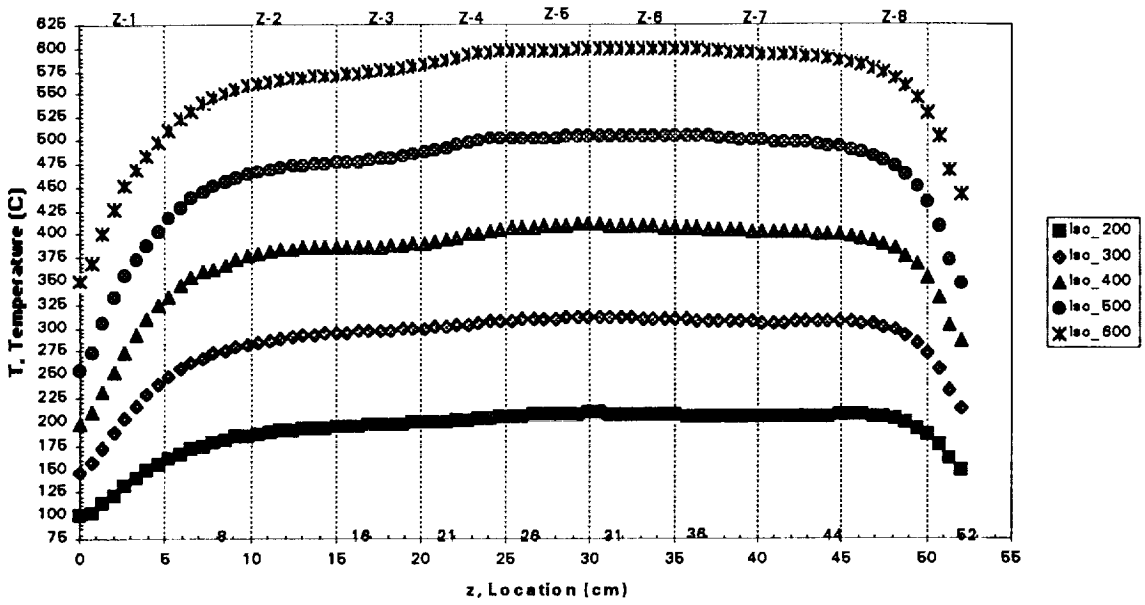

Figure 4 - Illustration of nearly isothermal profiles when all zones are set to the same temperature.

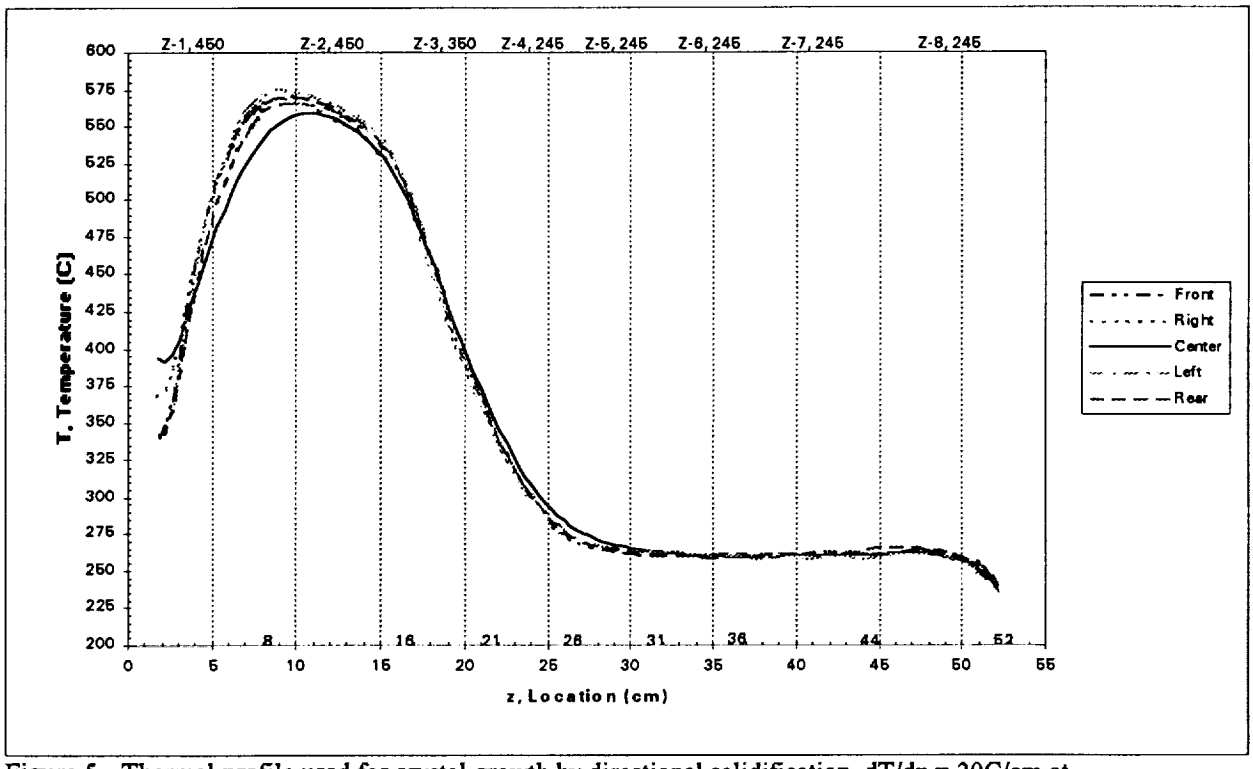

Figure 5 - Thermal profile used for crystal growth by directional solidification, dT/dz = 20C/cm at 16cm ≤ z ≤ 25cm.

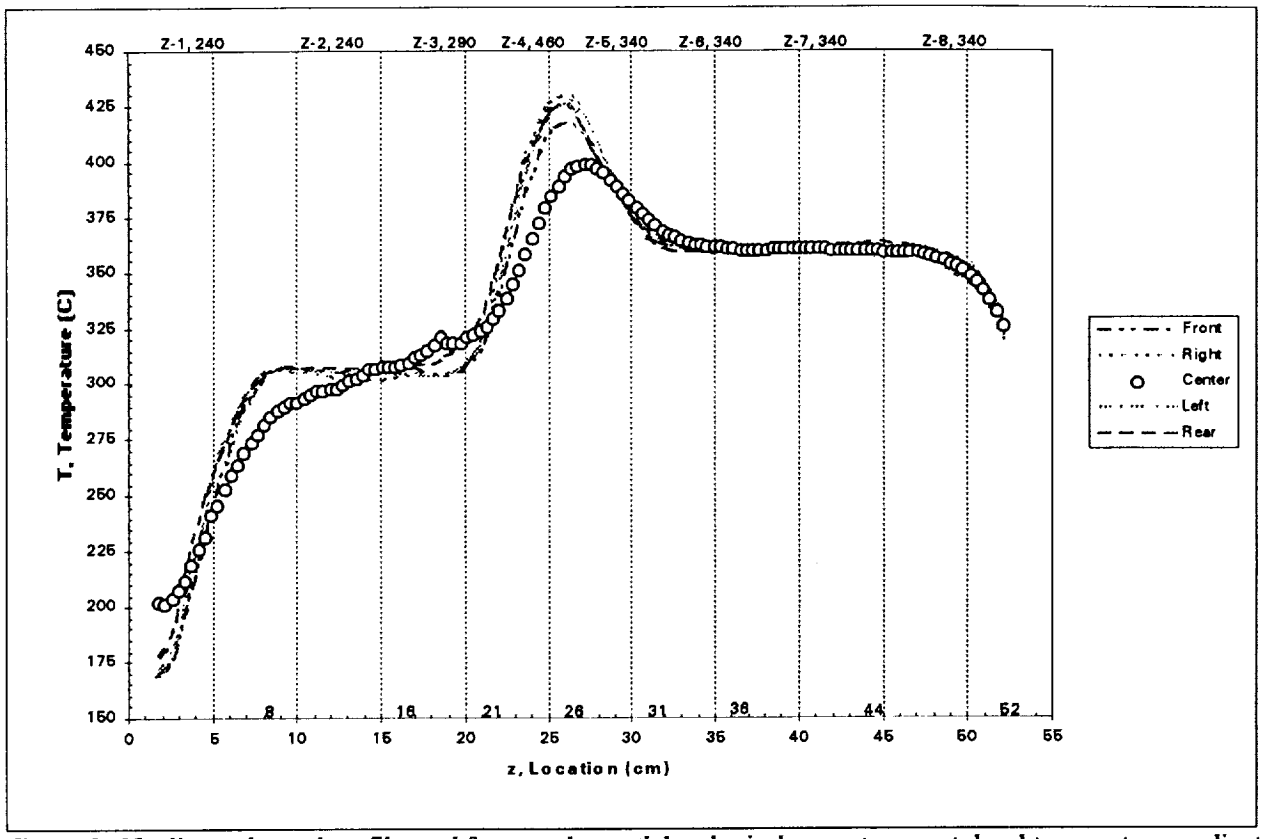

Figure 6 - Nonlinear thermal profile used for crystal growth by physical vapor transport, local temperature gradient at the centerline in the vicinity of 22cm $\leq z \leq$ 27cm is 17°C/cm.

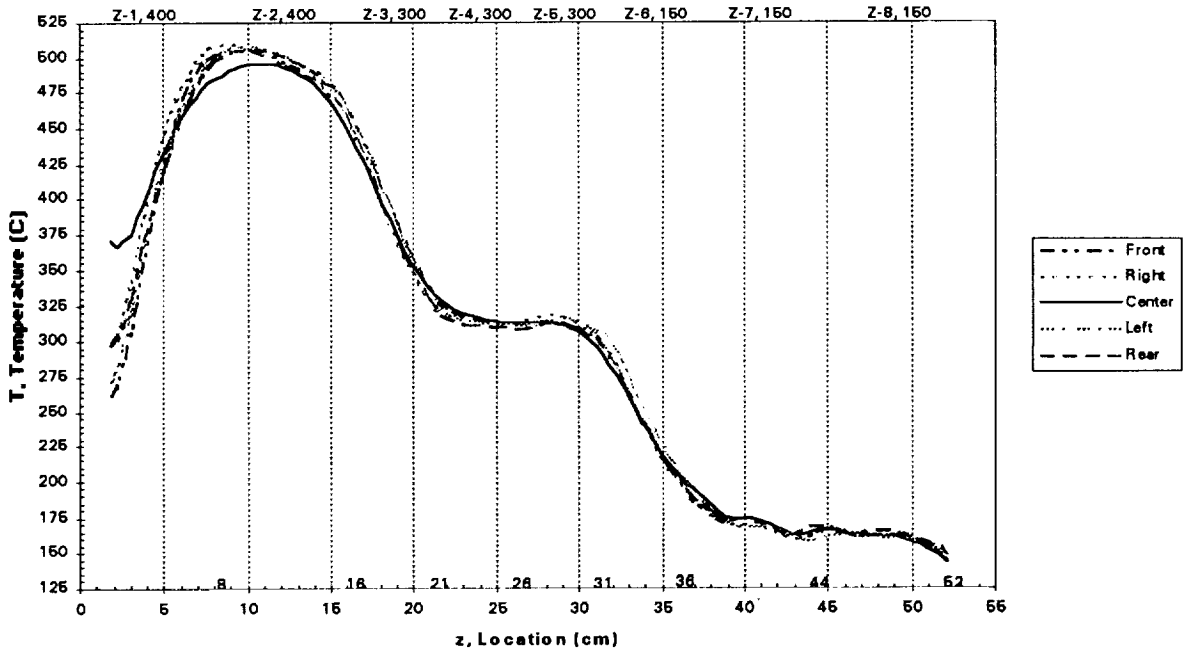

Figure 7 - Illustration of multiple gradient capability with isothermal region.

We have discussed in detail the furnace performance under no load conditions. The self-tuning temperature control is designed to account for zone to zone interactions. However, the thermal profile is preserved even with the presence of an ampoule for crystal growth. To show the response of the furnace under load conditions, we use the same condition as shown in Figure 5 for the linear thermal gradient. Note that the presence of an ampoule damps convective flows in the furnace. Figure 8 shows the measured thermal profile on the surface of an ampoule, 1.7 cm diameter and length 35.0 cm, containing lead bromide with a melting point of 373 ^{0} C. Comparison of the location of the solid-liquid interface to that indicated by the thermal profile shows reasonable agreement. This provides a calibration point for our thermal profile measurements. The result indicates that the control system accounts for thermal load conditions. Thus the thermal gradient projected by the furnace under no load conditions measured at the centerline corresponds to the surface input temperature at the ampoule wall. This implies that predetermined boundary conditions can be used as input to the furnace to study the dynamics of crystal growth. The ability of the self-tuning control system of the furnace to tailor thermal profiles represents an innovative concept that will find commercial applications for optimizing crystal growth conditions.

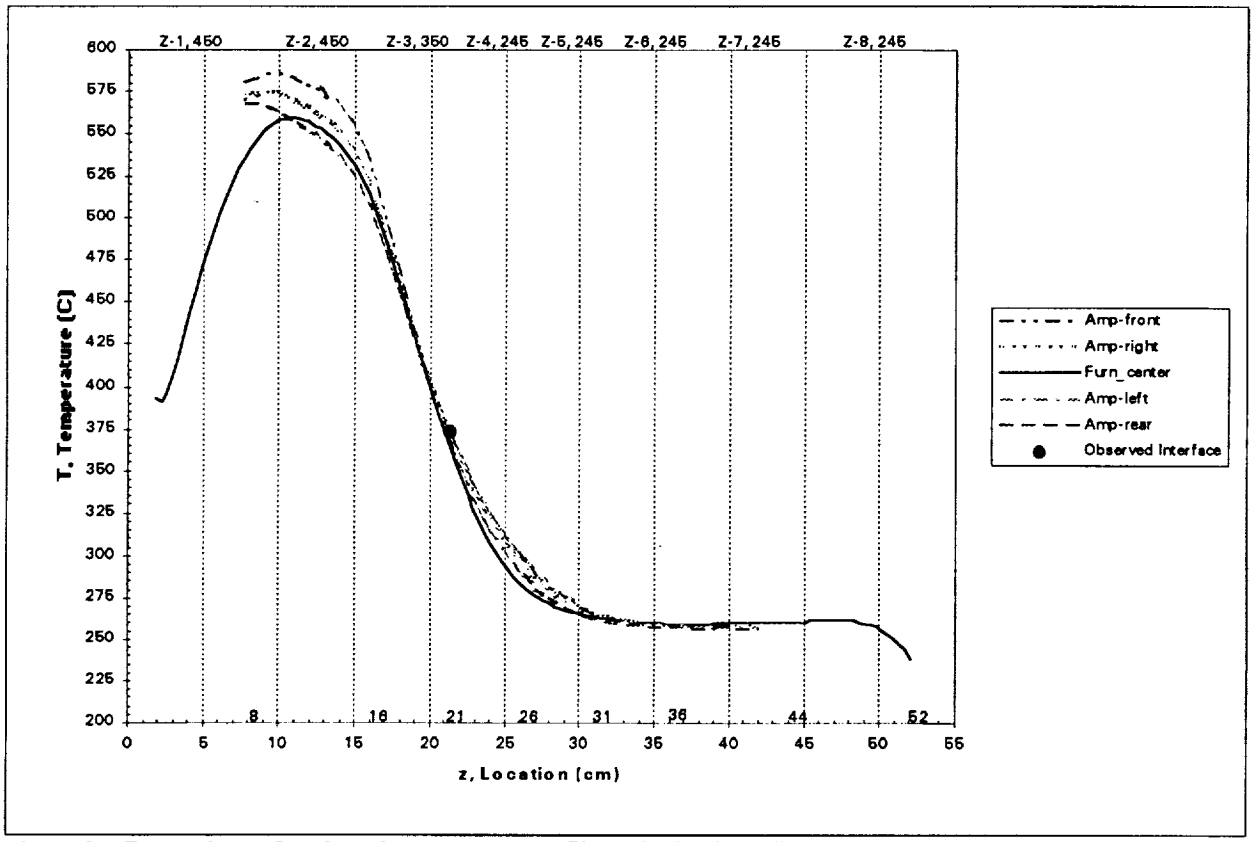

Figure 8 - Comparison of projected temperature profile under load conditions due to presence of ampoule filled with lead bromide, to no load conditions represented by centerline profile of the solid curve, dT/dz = 20^{0}C/cm 16cm $\leq$ z $\leq$ 25cm. Location of observed solid-liquid interface at the melting point of lead bromide, 373^{0}C, serves as a calibration point (see legend) for the system.

4.0 SUMMARY AND CONCLUSIONS

We have introduced an innovative concept of a transparent multizone furnace which uses a self-tuning temperature control system for the commercial application to crystal growth. This furnace operates in the temperature range of 25 - 750 °C . The self-tuning control accounts for zone to zone thermal interactions. The control system adjusts for thermal load, thus thermal profiles can be tailored prior to crystal growth and thermal gradients in the range of 2 °C/cm to 45°C/cm can be obtained. The operation of the furnace is based on the set-up of eight discrete temperatures over eight zones which result in a functional combination of heat flux distribution whose response is quantified from temperature profile measurements. The combination of the temperature profiles

for a given set-point temperature is shown to give temperature profiles of technological interest for the growth of crystals. These profiles include a range of thermal gradients for directional solidification applications, growth by vapor transport techniques, as well as multiple gradient applications. The innovation of the multizone crystal growth furnace is suited for crystal growth of a wide class of materials including, acousto-optic optoelectronics, photonics, low temperature semiconductors and organic materials. The hallmark of this furnace technology is its transparency and its ability to deliver precise thermal profiles.

5.0 ACKNOWLEDGEMENTS

We acknowledge the support of the Commercial Technology Office at NASA Lewis Research Center through Gary A.P. Horsham, Comm-Tech Program Manager. Technical discussions with N.B. Singh at Northrop Grumman and S. Trivedi at Brimrose Corporation of America are gratefully acknowledged.

6.0 REFERENCES

1.)Fu, Ta-Wei, Wilcox,W., "Influence of Insulation on Stability of Interface Shape and Position In The Vertical Bridgman-Stockbarger Technique,"Journal of Crystal Growth, 48, pp. 416-424, 1980.
2.)Ravishankar, R.S., and Fu, T.W. "Mathematical Modeling and Parametric Study of Heat Transfer in Bridgman Stockbarger Growth of Crystals," Journal of Crystal Growth, 62, pp. 425-432, 1983.
3.)Chin, Lih-Yen, Carlson, F. "Finite Element Analysis of Control of interface Shape in Bridgman Crystal Growth." Journal of Crystal Growth, 62, pp. 561-567, 1983
4.)Chang, Chong E. and Wilcox, W. R. "Control of Interface Shape in the Vertical Bridgman-Stockbarger Technique", Journal of Crystal Growth, 21, pp. 135-140, 1974
5.)Hartman,E., Schonherr, E. "Determination of Crystal Growth Rates from the Vapor by Relaxation," Journal of Crystal Growth, 51, pp. 140-142, 1981.
6.)E Schonherr, "Phenomenological Description of Crystal Growth From the Vapor" Journal of Crystal Growth, 57, pp. 493-498, 1982.
7.)Clyne, T.W. "Heat Flow in Controlled Directional Solidification of Metals, I Experimental Investigation",Journal of Crystal Growth 50, pp. 684-690, 1980.
8.)Clyne, T.W. , "Heat Flow in Controlled Directional Solidification of Metals, II Mathematical model", Journal of Crystal Growth 50, pp. 691-700, 1980.
9.)Batur, C., ,Sharpless, R.B., Duval, W.M.B., Singh, N.B., Rosenthal, B.N., "Identification and Control of a Multizone Crystal Growth Furnace," Journal of Crystal Growth, 119, pp. 371-380, 1992.
10.)Batur, C., Srinivasan, A., Duval, W.M.B., Singh, N.B.,"Control of Crystal Growth in Bridgman Furnace," Prog. Crystal Growth and Charact., 30, pp. 217-236, 1995.
11.)Lan,C.W., Yang, D.T., Ting, C.C., Chen, F.C.," A Tranparent Multizone Furnace For Crystal Growth and Flow Visualization,"Journal of Crystal Growth, 142, pp. 373-378, 1994.
12.)Srinivasan A., Batur C., Veillette R., "Projective Control Design for Multi-zone Crystal Growth Furnace", IEEE Transactions on Automatic Control System Technology, Vol. 2., No.2., pp. 142-148, 1994.
13.)Neumann, G., "Three Dimensional Numerical Simulation of Buoyancy-Driven Convection in Vertical Cylinders Heated from Below," Journal of Fluid Mechanics, 214, pp. 559-578, 1990.